An improved synthesis route to graphene for molecular sensor applications

Larisika, Melanie; Huang, Jingfeng; Knoll, Wolfgang; Nowak, Christoph; Tok, Alfred Iing Yoong

2012

Larisika, M., Huang, J., Tok, A., Knoll, W., & Nowak, C. (2012). An improved synthesis route to graphene for molecular sensor applications. Materials Chemistry and Physics, 136(2-3), 304-308.

https://hdl.handle.net/10356/96921

https://doi.org/10.1016/j.matchemphys.2012.08.003

An improved synthesis route to graphene for molecular sensor applications

Melanie Larisika[1,2], Jingfeng Huang[3], Alfred Tok[3], Wolfgang Knoll[1,2] and Christoph Nowak[1,2*]

[1] Austrian Institute of Technology (AIT) GmbH, Donau-City Str.1, Vienna, 1220, Austria.
[2] Centre for Biomimetic Sensor Science, 50 Nanyang Drive, Singapore, 637553, Singapore.
[3] School of Material Science and Engineering, Nanyang Technological University, 50 Nanyang Avenue, Singapore, 637553, Singapore.
** Corresponding author. Email: c.nowak@ait.ac.at*

Materials Chemistry and Physics Volume 136, Issues 2–3, 15 October 2012, Pages 304–30
http://dx.doi.org/10.1016/j.matchemphys.2012.08.003
http://www.sciencedirect.com/science/article/pii/S0254058412007110

Keywords:

Chemical synthesis; Monolayers; Semiconductors; Large Graphene Oxide

Highlights

- Improved synthesis of large monolayer Graphene Oxide
- Increased total yield of Graphene Oxide (25% yield)
- Remarkable lower sheet resistance and higher hole mobility
- Average size ~7 orders of magnitude larger than previously reported methods
- Characterization of large monolayer Graphene Oxide
- Demonstrated use in Field-Effect Transistor up to 100V

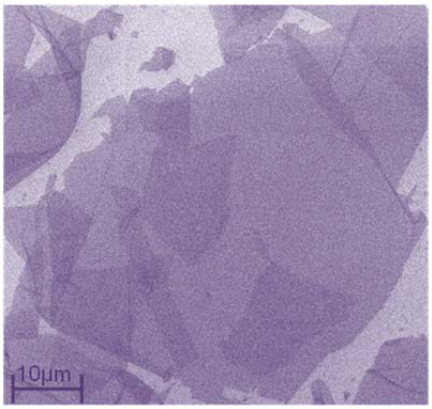

Figure: SEM image of a large GO sheet on SiO_2 substrate produced from the reported modified method.

Abstract

This article presents an improved graphene oxide synthesis method and its subsequent simple reduction technique with hydrazine vapour more efficiently to produce large area graphene flakes with a dramatic change in average sheet resistance of ~145kΩ/□ as compared to existing annealing methods. With the above characteristics, a high-performance and low-voltage operating graphene field-effect transistor (FET) was achieved with the potential to be used as detection platform for biomolecules.

Article Outline

1. Introduction

Graphene, a single-atom-thick and two-dimensional carbon nanomaterial[1], has attracted increasing attention in various applications including nano-electronics[2], energy storage[3], field-effect transistors (FETs)[4, 5] and sensors[6-11] because of its unique physical and electrical properties[12-14]. So far, single or few-layered graphene have been prepared by various methods including mechanical exfoliation ("Scotch-tape" method)[6, 9, 15], chemical vapour deposition (CVD)[1, 10] and chemical reduction of graphene oxide (GO)[7, 8]. The Scotch-tape method based on mechanical cleavage has main disadvantage due to low yield of graphene obtained. This makes it unsuitable for large-scale use. Efforts on chemical vapor deposition (CVD) have focused on growing films of graphene in large scale up to centimeter-sized graphene films on metallic substrate like Ni or Cu but the ability of transferring such films to other substrates still remains a cumbersome process[16]. Also, unacceptable uniformity of Ni-CVD[17] and self-limited monolayer formation of Cu-CVD[18] limits the applications of CVD based graphene, thus rendering it ineffective for biosensing applications. Moreover, synthesis of graphene by high temperature chemical vapour deposition (CVD) techniques is complicated, expensive and often time-consuming.

Chemical methods for preparing graphene oxide are highly suitable for low cost and large scale production of graphene. Previously reported reduction methods (refer Table 1) refer to using hydrazine vapour[19, 20] but it lead to only moderate electrical conductivity possibly due to inefficient reduction process. In other cases 20% H_2/Ar annealing at 800-1000^{o}C was used [20, 21] but this would be unsuitable for thermally unstable plastic materials. Besides using a facile and reproducible method appropriate for the large-scale production of GO, the reduction process of GO sheets can still be improved to make the final chip suitable for molecular sensing.

Table 1: Comparison of ultrathin electrodes prepared from various reduced GO sheets.

Process	Transparency @ 550nm (%)	sheet resistance (kΩ / □)
hydrazine reduction at 70 °C for 16h	98.3	145[a]
hydrazine reduction	95.4	19000[b]
hydrazine reduction at 80 °C	N.d.	4000[c]
hydrazine reduction at 80 °C for 24h	60-95	100000[d]
20% H2 800 °C, 2h	98.0	1005[e]
20% H2/Ar, 900 °C, 2h	98.1	413[e]
20% H2/Ar, 1000 °C, 2h	98.0	188[e]
1100 °C vacuum annealing, 3h	95.0	500[e]

N.d. = not determined

[a]Average sheet resistance obtained from our devices, refer to distribution in S5. [b]From ref.29 [c]From ref.24 [d]From ref.20 [e]From ref.17

Here, we report a modification of Hummers' method described by Su et al. 2009[20] that involves an easy to perform re-suspension step, resulting in readily exfoliated graphene oxide (GO) sheets with improvements in total yield. These sheets could be reduced by hydrazine vapour more effectively.
Our GO sheets, up to 3500 μm^2 in size, were deposited on appropriate SiO_2/Si wafer and the subsequent reduction process using hydrazine vapour resulted in remarkable lower sheet resistance and higher hole mobility of the devices, than from the original method[20]. No additional annealing step after hydrazine reduction was needed to achieve high conductivities of the graphene flakes. Electronic transfer measurements on our graphene devices indicate that they are very stable over a broad range of gate voltages (V_g). Thus our graphene FET operates at low-voltage making it suitable for molecular sensing applications.

Initially, we modified the graphene oxide (GO) synthesis method described by Su et al. 2009 by taking only large floating flakes after the ultra-sonication and oxidation steps for further processing. According to ref.[20], a graphite pre-oxidation procedure is needed to avoid incompletely oxidized graphite-core/GO-shell particles in the final product. In our case due to the large size of the natural graphite flakes (3-5mm), we also observed that the floating flakes were not fully oxidized, so GO sheets might be weakly attached to the graphite core.

In a typical synthesis, large flakes were collected after the main oxidation step, washed and re-suspended into 500 ml DI water by stirring overnight. Due to this mechanical movement, large GO flakes that were weakly adhered to the core peeled off. Since GO is soluble in water because of its carboxyl-and hydroxyl groups, exfoliation was achieved by this dilution step. In contrast to other exfoliation methods [20, 21], our technique did not involve ultra-sonication as we believe that ultra-sonication would lead to small size GO flakes.

2. Material and methods

2.1 Materials

Graphite flakes (3-5mm) were obtained from NGS Naturgraphit GmbH, Leinburg, Germany. Rest of the chemicals (research grade) were obtained from Sigma Aldrich, Pro Analysi and Merck. De-ionized water was used throughout the experiment.

2.2 Synthesis of Graphene Oxide

Graphene oxide (GO) sheets were prepared by the modified Hummers' method from natural graphite flakes (average size is 3-5mm). We modified the Hummers' method reported by Su et al.2009 in various steps. Briefly, 2g graphite flakes were mixed with concentrated H_2SO_4 (12ml) and stirred for 4-5 hours at 80 °C. After cooling to room temperature, the flakes were then ultra-sonicated for 1 hour and diluted with DI water (500ml) and left overnight. The mixture was filtered through porous filter (0.2μm) to obtained pre-oxidized graphite powders. The product was dried overnight in vacuum desiccator. The yield was 1.43g of pre-oxidized product (~71.3% yield).

The dried graphite powder was then added slowly into concentrated H_2SO_4 (120ml) and $KMnO_4$ (15g). The solution was stirred for 2 hrs at room temperature and then diluted with DI water (250ml) in an ice-bath and stir for another 2 hrs before final dilution with DI water (700ml). Shortly thereafter, H_2O_2 (20ml) was added into the mixture, resulting in a colour change to light yellow. The solution was kept overnight and then the next day only the upper portion of the mixture was collected, filtered and washed with 1:10 HCl aqueous solution to remove metal ions followed by 500 ml of DI water to remove the acid. Finally, the resulting solid was stirred overnight in DI water (500ml) to obtain a stock solution of GO. This solution was then centrifuged at 5000xg for 3 minutes and further purified by dialysis (cutoff 3000MW) against DI water for one week. After drying 0.49g of the product was obtained (~34.8%) meaning an overall yield of ~24.9% (compared with the starting material).

2.3 Reduction of Graphene Oxide

Silicon substrates were first cleaned with a standard RCA solution to remove undesired impurities. Subsequently, the cleaned SiO_2 substrates were modified with APTES self-assembled monolayers (SAMs), in order to enhance the adsorption of graphene oxide. Therefore, the substrates were immersed into a 1-2% APTES solution in ethanol for 1h, followed by extensively rinsing with absolute ethanol, before baking for 2 hours at 120 °C. Devices (300nm silicon oxide layer chips) were dip-coated with GO solution (1.3 mg/ml) for 1 hour, followed by thoroughly rinsing with DI water and drying with N_2. For the hydrazine vapour reduction, samples were put into glass petri dishes and 500 μl of 98% hydrazine monohydrate was placed in the edge of the petri dish. The samples were kept in the sealed petri dish at 70 °C for 16h.

2.4 Characterization techniques

SEM: Field Effect Scanning Electron Microscopy (FESEM) micrographs were taken using a JEOL JSM-7600F instrument operating at 1KeV.

AFM: Imaging of GO and rGO (reduced Graphene oxide) flakes by atomic force microscopy (AFM; Asylum Research AFP-3D) was performed with special emphasis on sheet thickness, morphological features, and lateral dimensions. All images were taken using tapping mode under ambient conditions and analyzed using WSxM Develop 3.3 software.

Raman: Raman spectra were measured in a WITec Alpha 300 confocal Raman microscopy system (with a laser wavelength of 532nm and a laser spot size of $1\mu m^2$). The Raman spectra were acquired using 10s integration time, with a laser power of 0.1mW. SERS spectra were analyzed using the software package WITec control 1.54 & WITec project 2.06.

XPS: X-ray Photoelectron Spectroscopy (XPS) analysis was performed on a VG ESCALAB 220i-XL with an Al Kα (1486.6eV) monochromatic X-ray source. Measured binding energy error is estimated to be within ±0.2eV.
Sheet resistance: Sheet resistance was measured using the four point probe method (AIT Instrument).
Electrical measurements: Electrical properties were monitored with a Keithley semiconductor parameter analyser, model 4200-SCS.

2.5 Graphene Oxide FET Fabrication

Field-effect transistor devices were fabricated by evaporating Au electrodes (80-100nm thick) with Cr adhesive layer (2-3nm thick) directly on top of the device using a hardmask. The obtained channel length (L) between source and drain electrodes are 60µm.

3. Results and discussion

3.1 SEM and AFM characterization

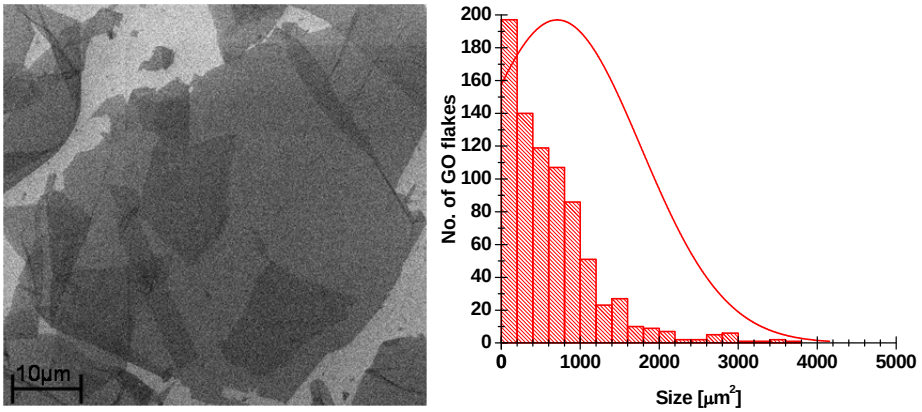

Figure 1: (left) SEM image of a large GO sheet on SiO_2 substrate produced from the modified method. (right) Size distribution of GO flakes. Solid curve indicates the Gaussian fit.

Figure 1 displays scanning electron microscopy (SEM) image of an ultra-large GO flake. The average size of the GO flakes obtained by our method is 700 µm^2, hence the GO membranes are of larger magnitude in area than those produced using previously reported methods[19].

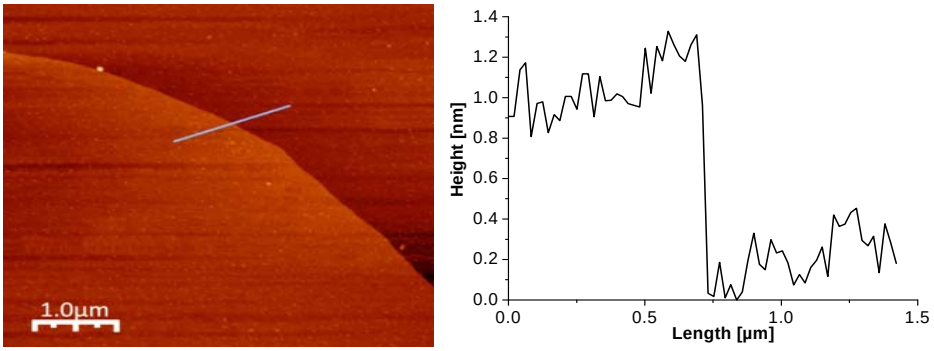

Figure 2: (left) AFM image of GO and (right) AFM height profile for the GO sheet.

Figure 2 shows a typical tapping mode AFM image of GO and rGO. The thicknesses of monolayer GO flakes are typically in the range of 0.7-1nm[21-24]. By the AFM height profile it is shown that the thickness for the GO sheet obtained by our modified method is ~ 1nm, suggesting that mono-layered GO could be proven over a large area. The AFM profile for rGO is observed as 0.8 nm. This is equivalent to the thickness observed by other references enclosed [25, 26]

3.2 Raman and XPS characterization

As shown in Figure S1 the Raman spectrum of GO displays two prominent peaks at 1341cm^{-1} and 1601cm^{-1}, which correspond to the well-documented D and G bands. At 2680 cm^{-1} the well documented 2D band appears originating from a double-resonance process of the D band at 1340 cm^{-1}.The Raman spectrum of rGO also exhibits both D and G bands (at 1330 and 1595 cm^{-1}, respectively). However, the D/G intensity ratio is increased in comparison with that of the GO spectrum.

In summary, the Raman spectral results described above are in good agreement with those reported by Stankovich[27], indicating that graphitization took place in rGO.

X-ray photoemission spectroscopic (XPS) measurements were performed for the as-prepared GO sheets and those after reduction with hydrazine vapour.

The C1s spectrum of GO (Figure S2) indicates the presence of two types of carbon bonds: C-C (284.5 eV) (composition = 46.5%), C=O (286.7 eV) (composition = 53.5%). After hydrazine reduction, the peak intensity of the C=O (composition = 10.7%) species is much smaller than those in the spectrum of GO, suggesting considerable de-oxygenation by the reduction process[28]. Also the composition of C-C increased to 72.3% in rGO (284.5eV). These values are consistent with a reduction of GO [27, 29, 30].

3.3 FET fabrication and electronic properties

Moreover, we tested the hydrazine reduced GO sheets with regards to their abilities to serve as conducting thin-film electrodes. Therefore bottom-gate operated transistors were easily fabricated without using elaborate electron-beam lithographic techniques by evaporating Au electrodes (100nm thick) directly on top of the selected rGO films that were previously deposited on 300nm SiO_2/Si substrates.

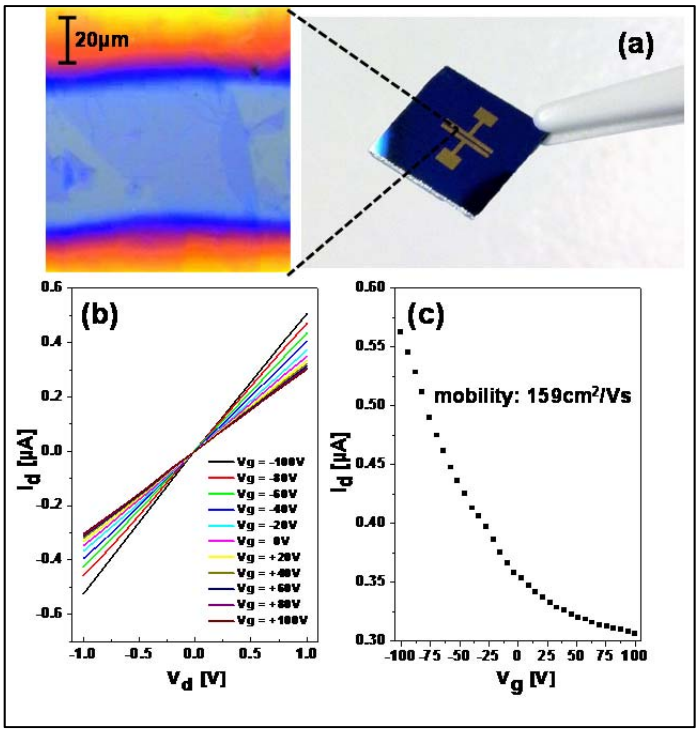

Figure 3: (a) Optical micrograph of the fabricated graphene device. (b) Output characteristics of the transistor device under different applied gate voltages. (c) Current – voltage transfer curve of bottom-gated graphene FET at a drain-source bias of V_d = 0.1V.

Figure 3a shows an optical micrograph of a typical fabricated device. The transfer characteristics were measured to evaluate the efficiency of the FET device. Figure 3b shows the output characteristics (drain current I_d vs. drain voltage V_d) of the SiO_2-gated graphene FETs at eleven different gate voltages (V_g). The device showed a clear increase in conductance as the gate voltage changed from +100V to -100V, indicating that the reduced GO films behaved as p-type semiconducting materials[24]. Figure 3c demonstrates the typical transfer characteristics (I_d-V_g) of the graphene field-effect transistor (FET) measured under ambient conditions (source-drain bias voltage Vds= 100 mV) and its effective field effect hole mobility is ~ 159 cm^2/Vs. In order to extract the field-effect mobility of holes, only selected GO sheets with suitable size (~ 20µm x 50µm) were used for the transistor measurements[20]. As per the above indicated flake area, a graphene coverage corresponding to a channel width of 500µm is assumed. The channel width (W) and length (L) were 4000 and 60µm, respectively. The hole mobility was calculated from the linear regime of the transfer characteristics using the equation $\mu = \left(\frac{L}{WC_{ox}V_d}\right)\left(\frac{\Delta I_d}{\Delta V_g}\right)$, where L and W are the channel length and width and C_{ox} the gate capacitance.

Figure S3 summarizes the distribution of the hole mobility of graphene FET chips (50 chips) on SiO_2/Si substrate. A Gaussian fit indicates an average hole mobility of 40 cm^2/Vs, at a drain bias of 100 mV, which is once again remarkably higher than the reported ones after hydrazine chemical reduction[20, 31] too. It is assumed, that by the improved graphene synthesis, the following hydrazine reduction process was carried out more effectively, leading to field-effect mobility values even comparable with those achieved with other methods like “alcohol vapour reduction” [32].

Table 1 compares the effect of different reduction methods on the resistance of GO transparent electrodes. Although a similar transparency (T = 95-98%, corresponding to 1 or 2 layer GO[20] of the

films are reported, the sheet resistance values vary notably. The average sheet resistance of the GO transparent electrode (T ~ 98%) (Figure S4) obtained by our modified method decreases dramatically to ~145 kΩ/□ thus making it suitable for molecular sensing. This is lower than the typical sheet resistance for hydrazine-reduced GO electrodes[24, 29, 33] and comparable with annealing at high temperature (188-1005 kΩ/□) [20]. Furthermore, it should be mentioned that at least 23% of the 298 graphene devices tested exhibit sheet resistances significant lower than 100 kΩ/□ (Figure S5).

4. Conclusion

In summary, our improved graphene oxide synthesis followed by simplified hydrazine vapour-assisted reduction led to enhanced electrical conductivity of graphene flakes, a sheet resistance of ~145 kΩ/□ (average observed over 298 chips), thus creating potential high-performance and low-voltage operating graphene devices applicable for future applications in the field of molecular detection.

References

[1] Y. Huang, X. Dong, Y. Shi, C.M. Li, L.-J. Li, P. Chen, Nanoelectronic biosensors based on CVD grown graphene, Nanoscale, 2 (2010) 1485-1488.
[2] D. Li, M.B. Muller, S. Gilje, R.B. Kaner, G.G. Wallace, Processable aqueous dispersions of graphene nanosheets, Nat. Nanotechnol., 3 (2008) 101-105.
[3] E. Yoo, J. Kim, E. Hosono, H. Zhou, T. Kudo, I. Honma, Large Reversible Li Storage of Graphene Nanosheet Families for Use in Rechargeable Lithium Ion Batteries, Nano Lett., 8 (2008) 2277-2282.
[4] A. Das, S. Pisana, B. Chakraborty, S. Piscanec, S.K. Saha, U.V. Waghmare, K.S. Novoselov, H.R. Krishnamurthy, A.K. Geim, A.C. Ferrari, Monitoring dopants by Raman scattering in an electrochemically top-gated graphene transistor, Nat. Nanotechnol., 3 (2008) 210.
[5] Y. Sui, J. Appenzeller, Screening and Interlayer Coupling in Multilayer Graphene Field-Effect Transistors, Nano Letters, 9 (2009) 2973-2977.
[6] F. Schedin, A.K. Geim, S.V. Morozov, E.W. Hill, P. Blake, M.I. Katsnelson, K.S. Novoselov, Detection of individual gas molecules adsorbed on graphene, Nat Mater, 6 (2007) 652-655.
[7] J.T. Robinson, F.K. Perkins, E.S. Snow, Z. Wei, P.E. Sheehan, Reduced Graphene Oxide Molecular Sensors, Nano Letters, 8 (2008) 3137-3140.
[8] Q. He, H.G. Sudibya, Z. Yin, S. Wu, H. Li, F. Boey, W. Huang, P. Chen, H. Zhang, Centimeter-Long and Large-Scale Micropatterns of Reduced Graphene Oxide Films: Fabrication and Sensing Applications, ACS Nano, 4 (2010) 3201-3208.
[9] Y. Ohno, K. Maehashi, Y. Yamashiro, K. Matsumoto, Electrolyte-Gated Graphene Field-Effect Transistors for Detecting pH and Protein Adsorption, Nano Letters, 9 (2009) 3318-3322.
[10] X.C. Dong, D.C. Fu, W.J. Fang, Y.M. Shi, P. Cheng, L.J. Li, Doping Single-Layer Graphene with Aromatic Molecules, Small, 5 (2009) 1422-1426.
[11] P.K. Ang, W. Chen, A.T.S. Wee, K.P. Loh, Solution-Gated Epitaxial Graphene as pH Sensor, Journal of the American Chemical Society, 130 (2008) 14392-14393.
[12] A.K. Geim, K.S. Novoselov, The rise of graphene, Nat Mater, 6 (2007) 183-191.
[13] C.N.R. Rao, A.K. Sood, K.S. Subrahmanyam, A. Govindaraj, Graphene: The New Two-Dimensional Nanomaterial, Angewandte Chemie International Edition, 48 (2009) 7752-7777.
[14] M. Ishigami, J.H. Chen, W.G. Cullen, M.S. Fuhrer, E.D. Williams, Atomic Structure of Graphene on SiO2, Nano Letters, 7 (2007) 1643-1648.
[15] T. Cohen-Karni, Q. Qing, Q. Li, Y. Fang, C.M. Lieber, Graphene and Nanowire Transistors for Cellular Interfaces and Electrical Recording, Nano Letters, 10 (2010) 1098-1102.
[16] C.-H. Lu, H.-H. Yang, C.-L. Zhu, X. Chen, G.-N. Chen, A Graphene Platform for Sensing Biomolecules, Angewandte Chemie International Edition, 48 (2009) 4785-4787.
[17] B. Dai, L. Fu, L. Liao, N. Liu, K. Yan, Y. Chen, Z. Liu, High-quality single-layer graphene via reparative reduction of graphene oxide, Nano Research, 4 (2011) 434-439.
[18] X. Li, W. Cai, J. An, S. Kim, J. Nah, D. Yang, R. Piner, A. Velamakanni, I. Jung, E. Tutuc, S.K. Banerjee, L. Colombo, R.S. Ruoff, Large-Area Synthesis of High-Quality and Uniform Graphene Films on Copper Foils, Science, 324 (2009) 1312-1314.
[19] Z. Luo, Y. Lu, L.A. Somers, A.T.C. Johnson, High Yield Preparation of Macroscopic Graphene Oxide Membranes, J. Am. Chem. Soc., 131 (2009) 898-899.
[20] C.-Y. Su, Y. Xu, W. Zhang, J. Zhao, X. Tang, C.-H. Tsai, L.-J. Li, Electrical and Spectroscopic Characterizations of Ultra-Large Reduced Graphene Oxide Monolayers, Chemistry of Materials, 21 (2009) 5674-5680.
[21] D.C. Marcano, D.V. Kosynkin, J.M. Berlin, A. Sinitskii, Z. Sun, A. Slesarev, L.B. Alemany, W. Lu, J.M. Tour, Improved Synthesis of Graphene Oxide, ACS Nano, 4 (2010) 4806-4814.
[22] S. Stankovich, D.A. Dikin, R.D. Piner, K.A. Kohlhaas, A. Kleinhammes, Y. Jia, Y. Wu, S.T. Nguyen, R.S. Ruoff, Synthesis of graphene-based nanosheets via chemical reduction of exfoliated graphite oxide, Carbon, 45 (2007) 1558-1565.
[23] L. Gao, J.R. Guest, N.P. Guisinger, Epitaxial Graphene on Cu(111), Nano Letters, 10 (2010) 3512-3516.
[24] S. Gilje, S. Han, M. Wang, K.L. Wang, R.B. Kaner, A Chemical Route to Graphene for Device Applications, Nano Letters, 7 (2007) 3394-3398.
[25] E.-Y. Choi, T.H. Han, J. Hong, J.E. Kim, S.H. Lee, H.W. Kim, S.O. Kim, Noncovalent functionalization of graphene with end-functional polymers, Journal of Materials Chemistry, 20 (2010) 1907-1912.
[26] J. Liu, Y. Li, Y. Li, J. Li, Z. Deng, Noncovalent DNA decorations of graphene oxide and reduced graphene oxide toward water-soluble metal-carbon hybrid nanostructures via self-assembly, Journal of Materials Chemistry, 20 (2010) 900-906.
[27] S. Stankovich, R.D. Piner, X. Chen, N. Wu, S.T. Nguyen, R.S. Ruoff, J. Mater. Chem., 16 (2006) 155.
[28] Y. Xu, H. Bai, G. Lu, C. Li, G. Shi, Flexible Graphene Films via the Filtration of Water-Soluble Noncovalent Functionalized Graphene Sheets, Journal of the American Chemical Society, 130 (2008) 5856-5857.
[29] G. Eda, G. Fanchini, M. Chhowalla, Large-area ultrathin films of reduced graphene oxide as a transparent and flexible electronic material, Nat Nano, 3 (2008) 270-274.

[30] H.A. Becerril, J. Mao, Z. Liu, R.M. Stoltenberg, Z. Bao, Y. Chen, Evaluation of Solution-Processed Reduced Graphene Oxide Films as Transparent Conductors, ACS Nano, 2 (2008) 463.
[31] C. Gomez-Navarro, R.T. Weitz, A.M. Bittner, M. Scolari, A. Mews, M. Burghard, K. Kern, Electronic Transport Properties of Individual Chemically Reduced Graphene Oxide Sheets, Nano Letters, 7 (2007) 3499-3503.
[32] C.-Y. Su, Y. Xu, W. Zhang, J. Zhao, A. Liu, X. Tang, C.-H. Tsai, Y. Huang, L.-J. Li, Highly Efficient Restoration of Graphitic Structure in Graphene Oxide Using Alcohol Vapors, ACS Nano, 4 (2010) 5285-5292.
[33] L.J. Cote, F. Kim, J. Huang, Langmuir−Blodgett Assembly of Graphite Oxide Single Layers, J. Am. Chem. Soc., 131 (2009) 1043-1049.